Mitigation of Coronal Hole Obscuration for Open Flux Estimates

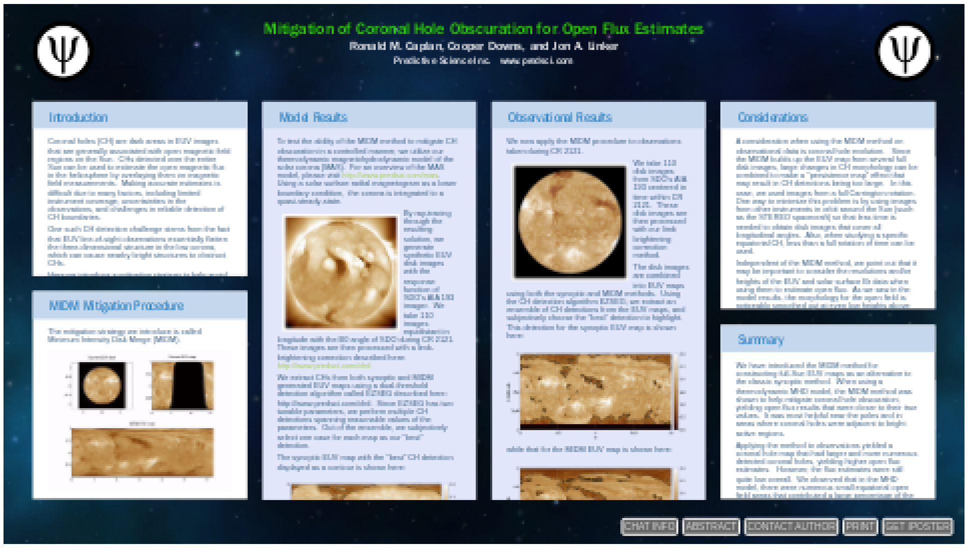

Ronald M. Caplan, Cooper Downs, and Jon A. Linker

Predictive Science Inc. www.predsci.com

PRESENTED AT:

AGU FALL MEETING

Online Everywhere | 1–17 December 2020

INTRODUCTION

Coronal holes (CH) are dark areas in EUV images that are generally associated with open magnetic field regions on the Sun. CHs detected over the entire Sun can be used to estimate the open magnetic flux in the heliosphere by overlaying them on magnetic field measurements. Making accurate estimates is difficult due to many factors, including limited instrument coverage, uncertainties in the observations, and challenges in reliable detection of CH boundaries.

One such CH detection challenge stems from the fact that EUV line-of-sight observations essentially flatten the three-dimensional structure in the low corona, which can cause nearby bright structures to obstruct CHs.

Here we introduce a mitigation strategy to help avoid the effects of CH obscuration.

To test the strategy, we use a global thermodynamic MHD model of the corona to generate synthetic EUV images for a multitude of observer locations (chosen to mimic the view of SDO over the solar rotation) and combine them into a full-Sun synoptic EUV map. The EUV map is made in both a standard synoptic manner, and in the new mitigation strategy method. CH maps are then extracted using an established detection algorithm and are compared to the model's true open field.

We then apply the procedure to SDO observations in the same time period, and explore the effects of the mitigation strategy on the CHs and open flux measurements derived from them.

We use Carrington rotation (CR) 2101 for our example case, and compare results from both the large equatorial coronal hole appearing in the middle of the CR, as well as those over the full Sun.

Issues such as CH evolution during the rotation, and synchronizing the effective EUV image height to the height of the magnetic field values are discussed.

MIDM MITIGATION PROCEDURE

The mitigation strategy we introduce is called Minimum Intensity Disk Merge (MIDM).

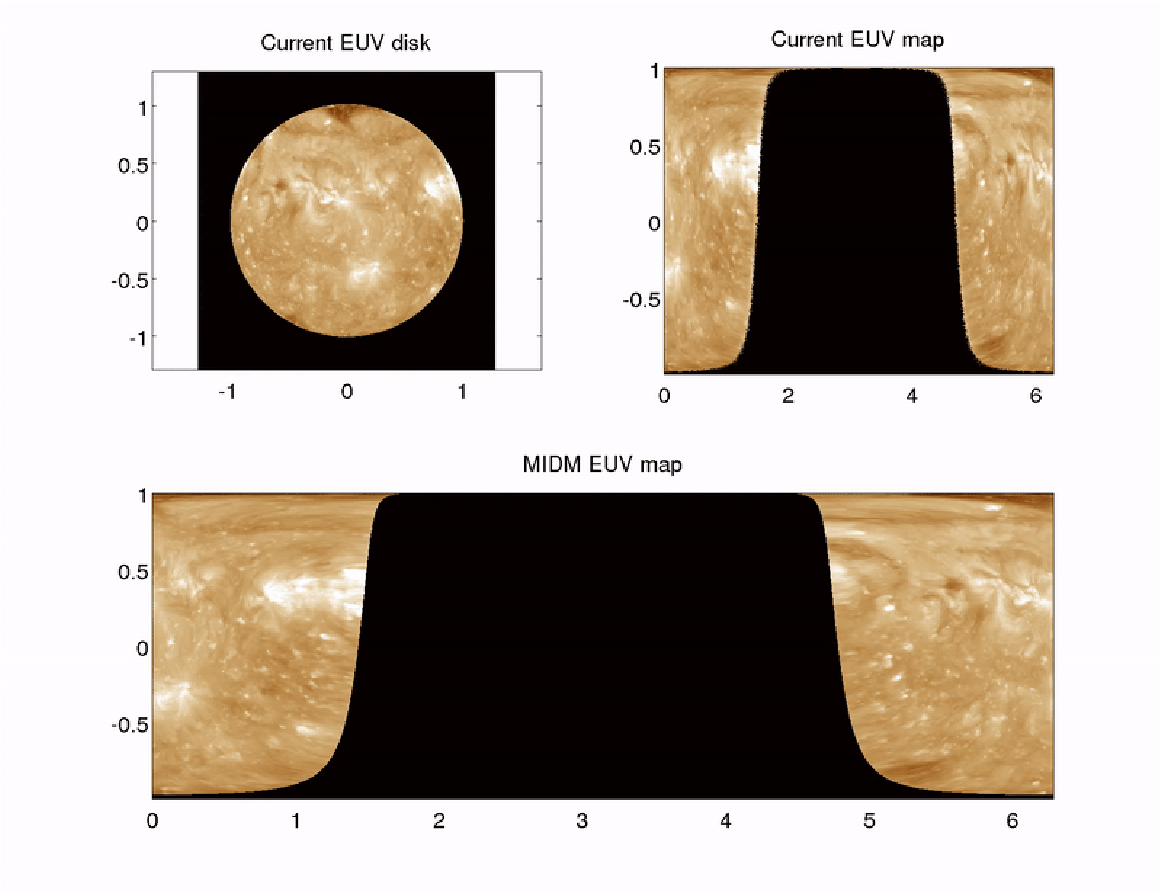

It is an alternative method to combine multiple EUV disk images into a full-Sun map. Instead of using central weighted latitude strips as in a synoptic map, MIDM takes full disk images and merges them based on which pixels in the overlap exhibit the minimum intensity. This allows any CH area observed at any vantage point to be seen in the final map.

Due to geometric distortions and lower fidelity data near the limbs, we implement a two-limit scheme on the data to be used. The first limit (`merge_mulimit`) defines what is considered "good" data for use in merging overlapping regions and is set in terms of `cos(theta)` where `theta` is the angle from disk center. The second limit (`mulimit`) defines what is considered "good enough" data outside of overlapping regions (here we set `merge_mulimit=0.25882` and `mulimit=0.1`). This allows data to be extended close to the poles, but only retain better data for most of the map area. It is also useful for avoiding salt-and-pepper dark pixels in observational data that is noisy near the limb from appearing in the final map. We note that the method does introduce some areas where "good" and "good enough" data are merged.

Given a set of disk images, for each current disk image projected onto a theta-phi map (`EUV_MAP`), the algorithm is described as follows.

Given index sets `I_data, I_nodata, I_data_in_mulimit, I_data_in_merge_mulimit` for the current `EUV_MAP`, we set:

```
I_data_good = I_data_in_merge_mulimit
I_data_bad  = I_data_in_mulimit & ~I_data_in_merge_mulimit

I_data_good_unique = I_data_good & I_final_nodata
I_data_bad_unique  = I_data_bad  & I_final_nodata

I_merge_good = (EUV_MAP < EUV_FINAL_MAP) & I_data_good & I_final_data
I_merge_bad  = (EUV_MAP < EUV_FINAL_MAP) & I_data_bad  & I_final_data_bad
```

```
EUV_FINAL_MAP(I_data_good_unique) = EUV_MAP(I_data_good_unique)
EUV_FINAL_MAP(I_data_bad_unique)  = EUV_MAP(I_data_bad_unique)
EUV_FINAL_MAP(I_merge_good)       = EUV_MAP(I_merge_good)
EUV_FINAL_MAP(I_merge_bad)        = EUV_MAP(I_merge_bad)

I_final_data     = I_final_data | I_data_good_unique | I_data_bad_unique | I_merge_good
| I_merge_bad
I_final_data_bad = I_final_data_bad | I_data_bad_unique | I_merge_bad
```

This sequence is repeated for each disk image to build up the final map (EUV_FINAL_MAP).

MODEL RESULTS

To test the ability of the MIDM method to mitigate CH obscuration in a controlled manner, we utilize our thermodynamic magnetohydrodynamic model of the solar corona (MAS). For an overview of the MAS model, please visit http://www.predsci.com/mas (http://www.predsci.com/mas). Using a solar surface radial magnetogram as a lower boundary condition, the corona is integrated to a quasi-steady-state.

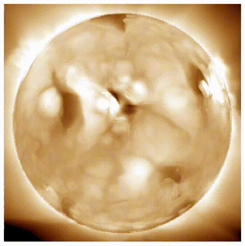

By ray-tracing through the resulting solution, we generate synthetic EUV disk images with the response function of SDO's AIA 193 imager. We take 110 images equidistant in longitude with the B0 angle of SDO during CR 2101. These images are then processed with a limb-brightening correction described here: http://www.predsci.com/chd (http://www.predsci.com/chd)

We extract CHs from both synoptic and MIDM generated EUV maps using a dual-threshold detection algorithm called EZSEG described here: http://www.predsci.com/chd. Since EZSEG has two tunable parameters, we perform multiple CH detections spanning reasonable values of the parameters. Out of the ensemble, we subjectively select one case for each map as our "best" detection.

The synoptic EUV map with the "best" CH detection displayed as a contour is shown here:

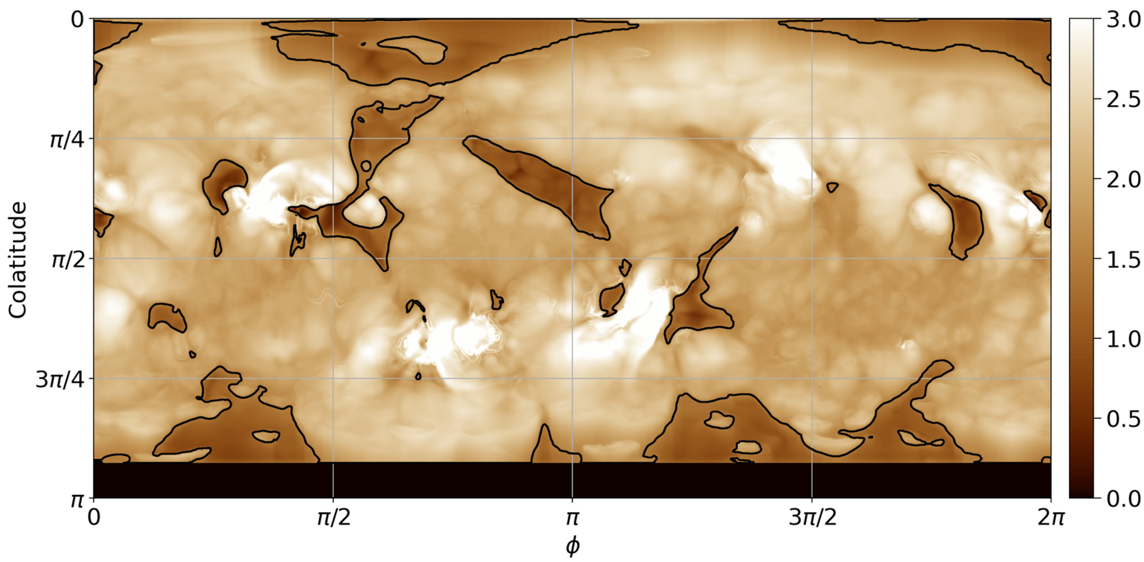

and the map for the MIDM method is shown here:

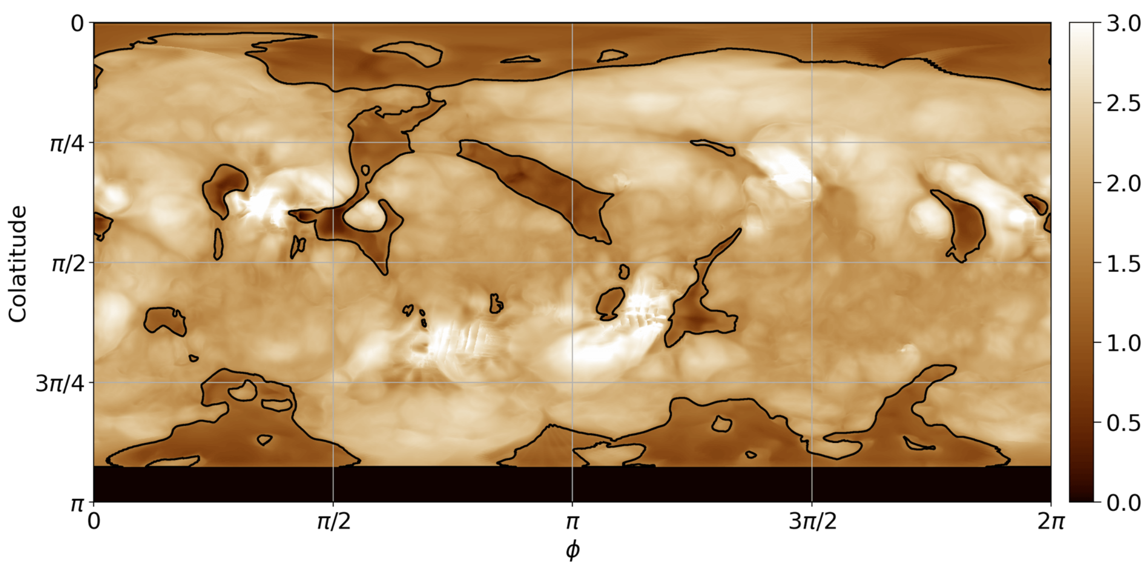

We see that the MIDM EUV map avoids the CH obscuration near the poles, as well as some near active regions.

To compute open flux estimates, we overlay the CHs on the Br magnetogram used in the model. This magnetogram was taken from the JSOC's pole-filled CR 2101 HMI synoptic map, but with the poles modified to have parasitic polarities, and the map smoothed to the model resolution. The map is show here:

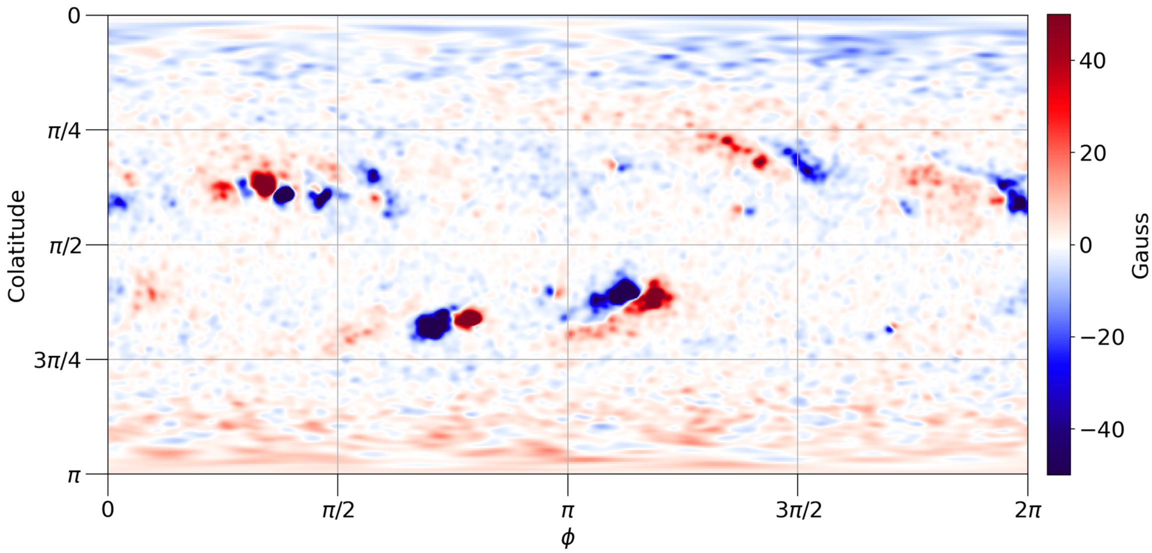

Overlaying the CH from the synoptic EUV map, yields

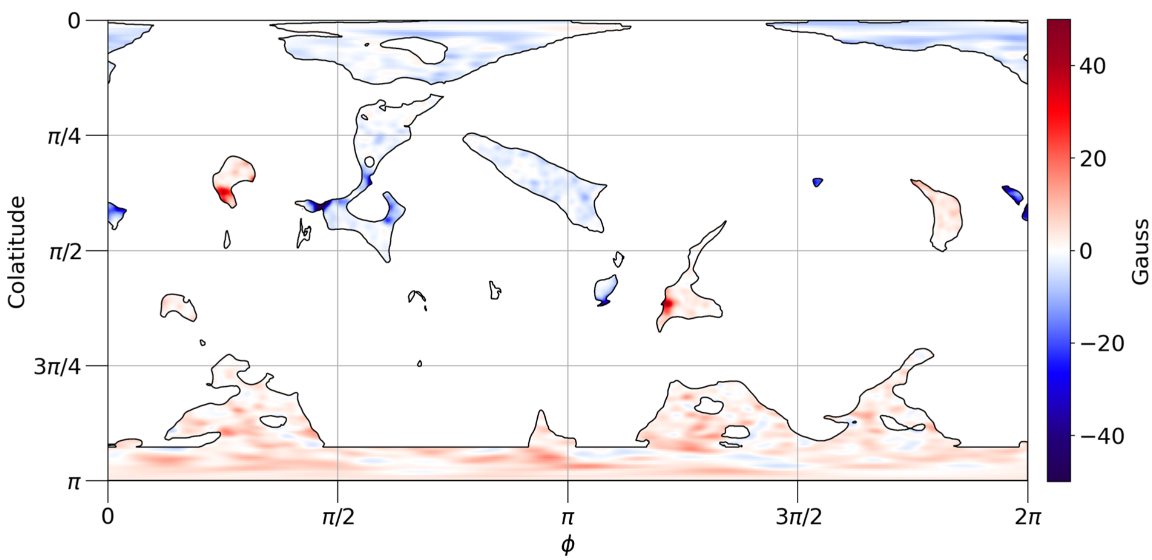

while overlaying the CH from the MIDM EUV map yields

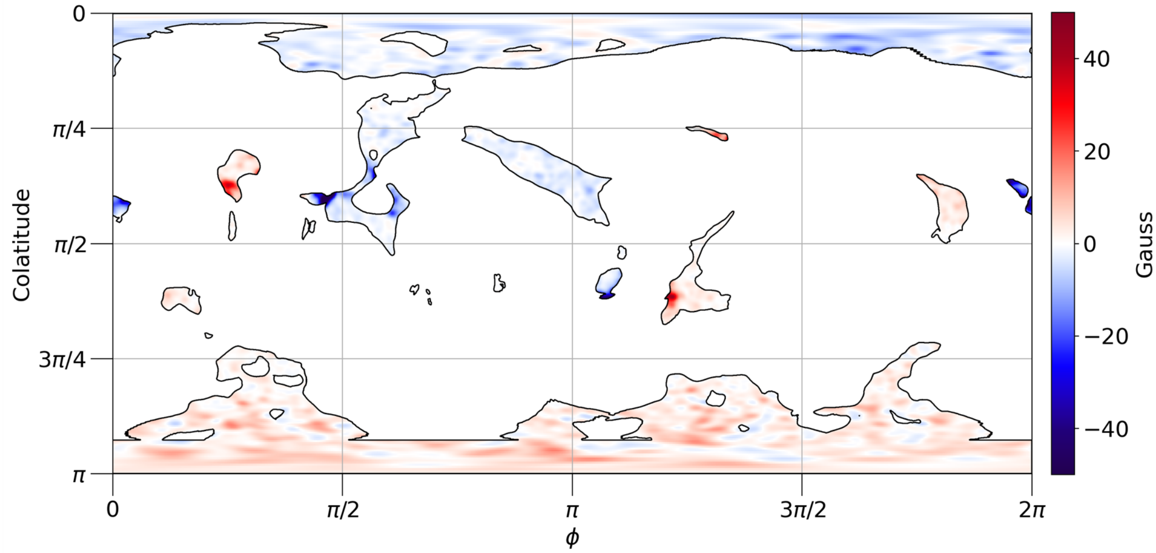

The following two figures show the percentage of open flux within each CH on the map for the synoptic and MIDM EUV maps respectively:

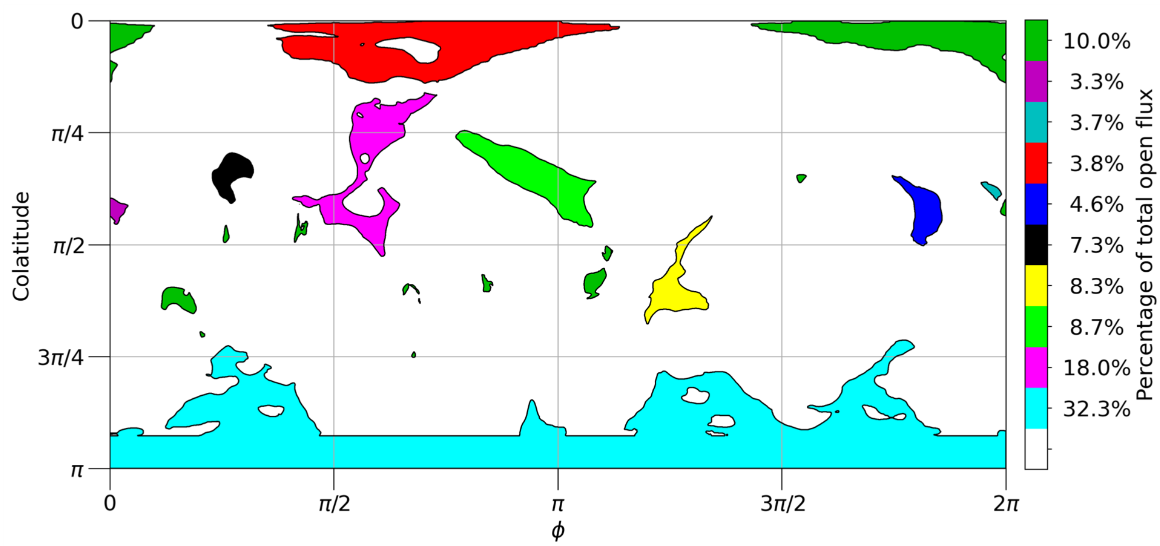

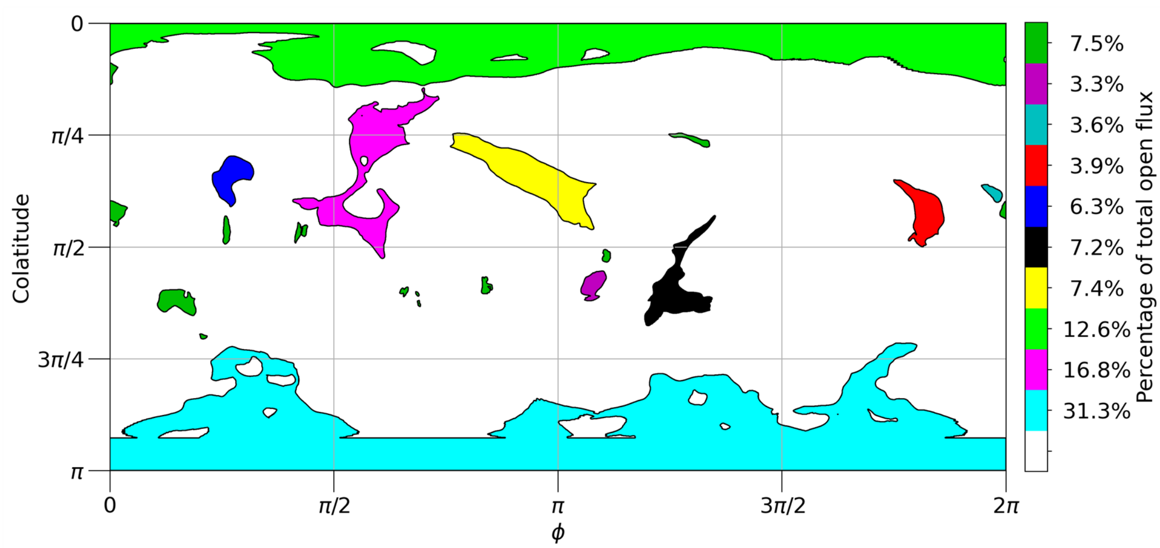

A great advantage of using a MHD model is that the true open field can be easily computed by tracing field lines through the coronal solution. This allows us to compare the areas and fluxes computed with the EUV-derived CHs to the true values of the model. The percentage flux per "CH" of the true open field is shown here:

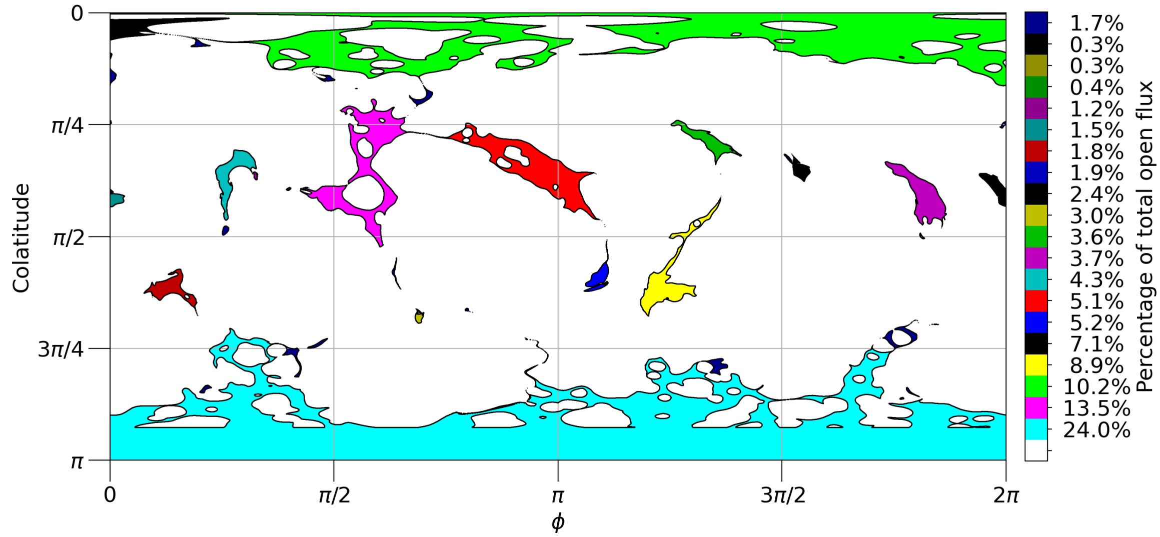

We see that the OF areas are smaller but with more structure. Also, several small areas exist that are not detected in the EUV maps.

One reason for the qualitatively different structure of the open field areas compared to the CH areas can be attributed to the EUV images being derived from a 3D integration in the low corona, yielding an image that has an "effective" height above the solar surface. This height (for the model) can be estimated to be r=1.02 Rs. To see this effect, we plot the OF of the model at different heights (r=1.00, r=1.01, and r=1.02), and see that the OF at r=1.02 matches more closely to the CHs derived from the EUV maps:

r=1.00

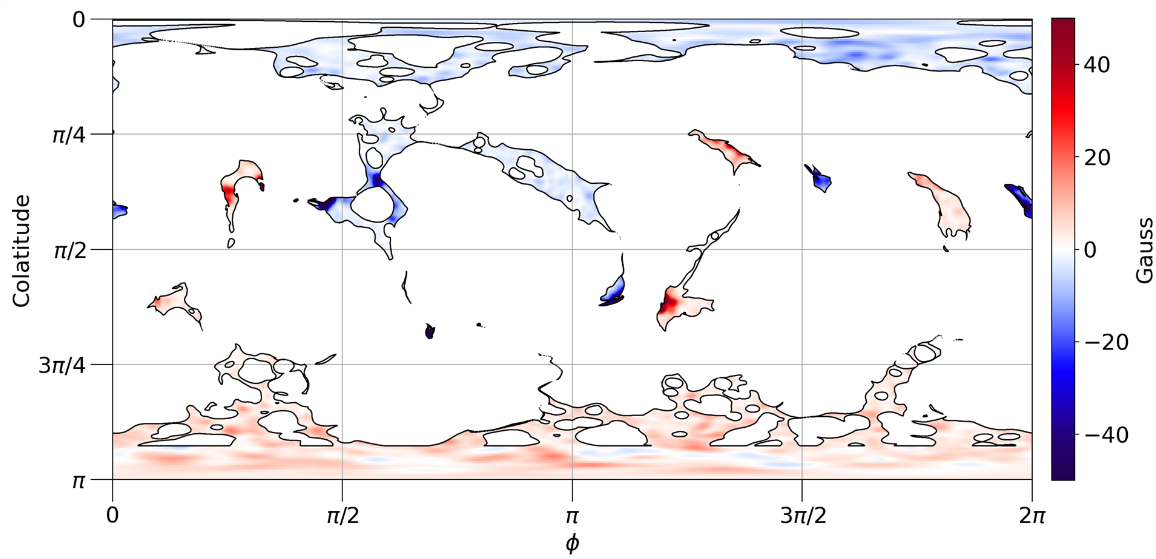

r=1.01

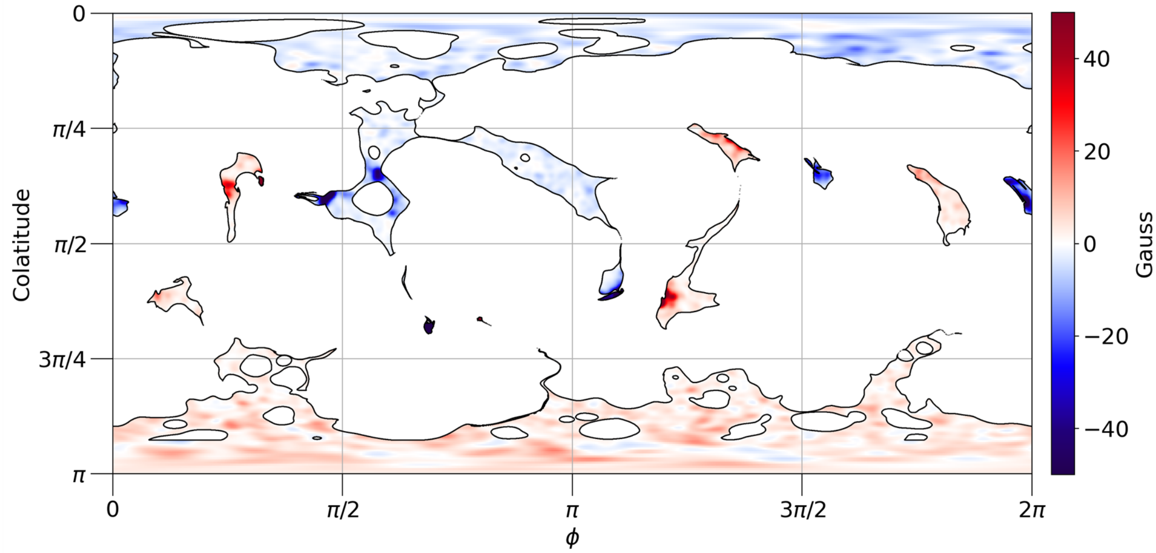

r=1.02

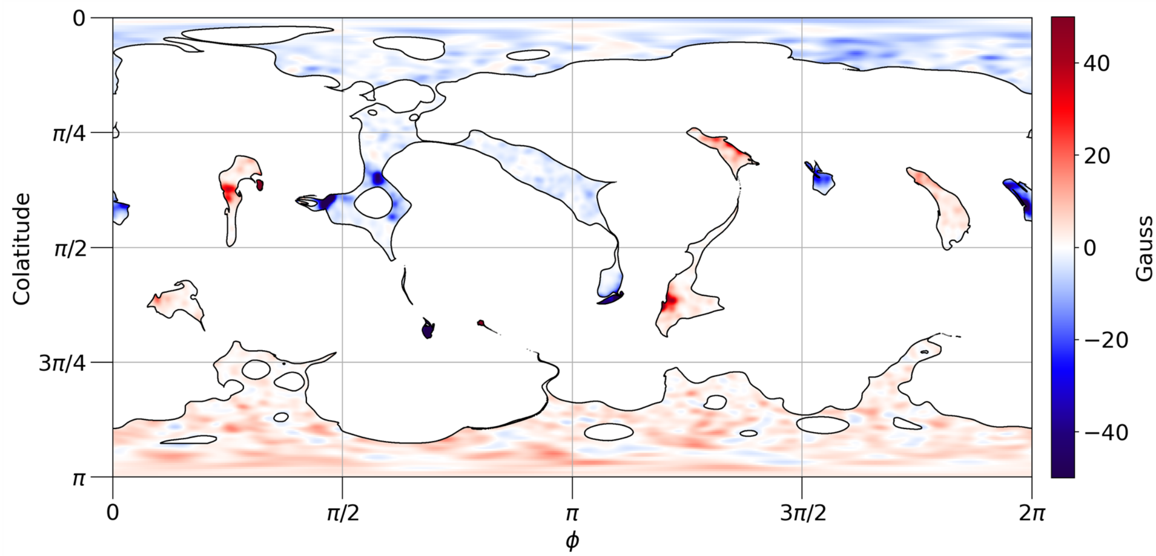

The Br in all the above plots are at the solar surface. The effect of using this field with open field maps at higher heights is discussed below.

The open flux results for only the central equatorial CH are shown here:

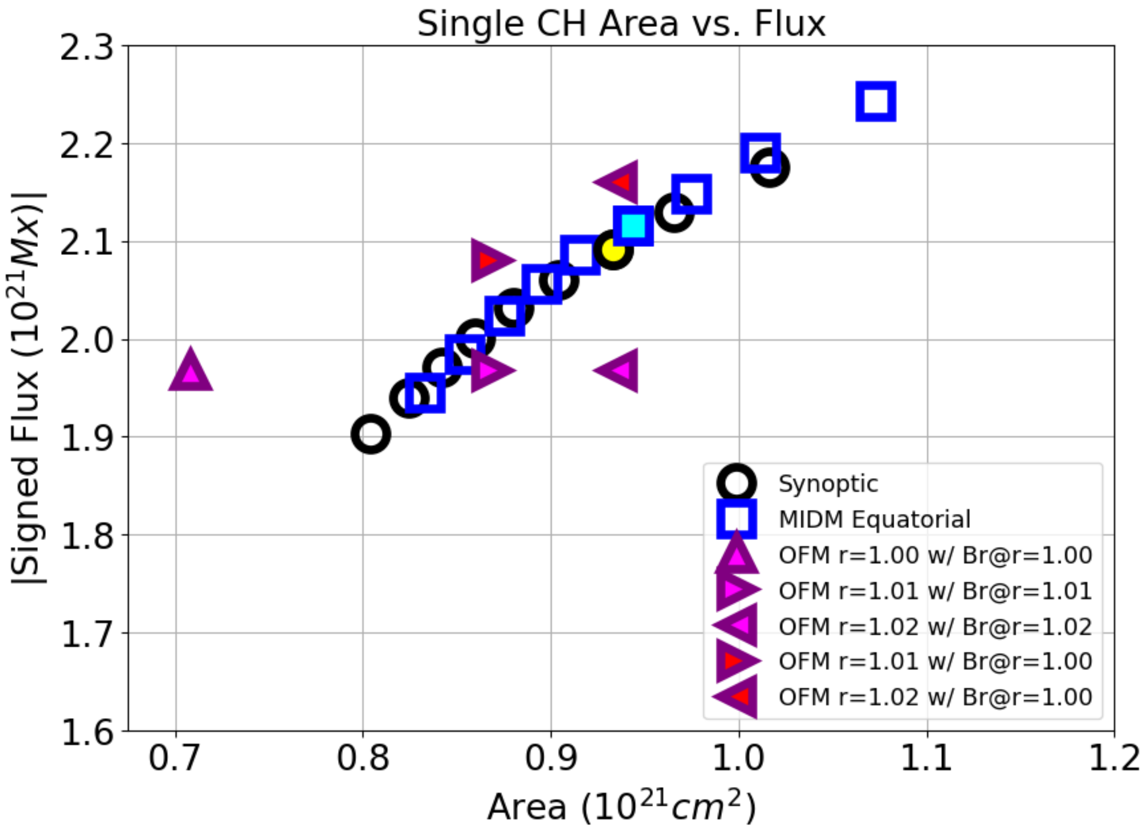

The yellow-filled circle and the cyan-filled square are the selected "best" CH detections of the synoptic and MIDM EUV maps respectively. We see that, for this individual CH, the results from the synoptic and MIDM EUV maps are similar. This is expected as there are no bright regions near the CH, and it is centrally located on the disk.

We also see that the true open field area is smaller than all reasonable CH detections, and the open flux is lower than both "best" detections. However, the area of the open field at r=1.02 (the effective EUV height) matches closely with our "best" CH detections, but with a lower open flux. Using (incorrectly) the surface magnetic field with the open field at r=1.02, yields results (shown as red-filled triangles) very close to the "best" CH detections. This shows that using a surface magnetic field with EUV CH detections may yield open flux estimates that are somewhat higher than the true open flux.

For the full-Sun, in order to be able to properly compare all results, we limit the open field maps in latitude at the southern pole to match the area of missing data in the EUV maps. In all cases, we assume the missing polar area is open field. This effect is small as the open flux between the full model open field with or without the latitude limit are within 99.9%.

The open flux (shown in terms of extrapolated IMF values at 1 AU) is shown versus area here:

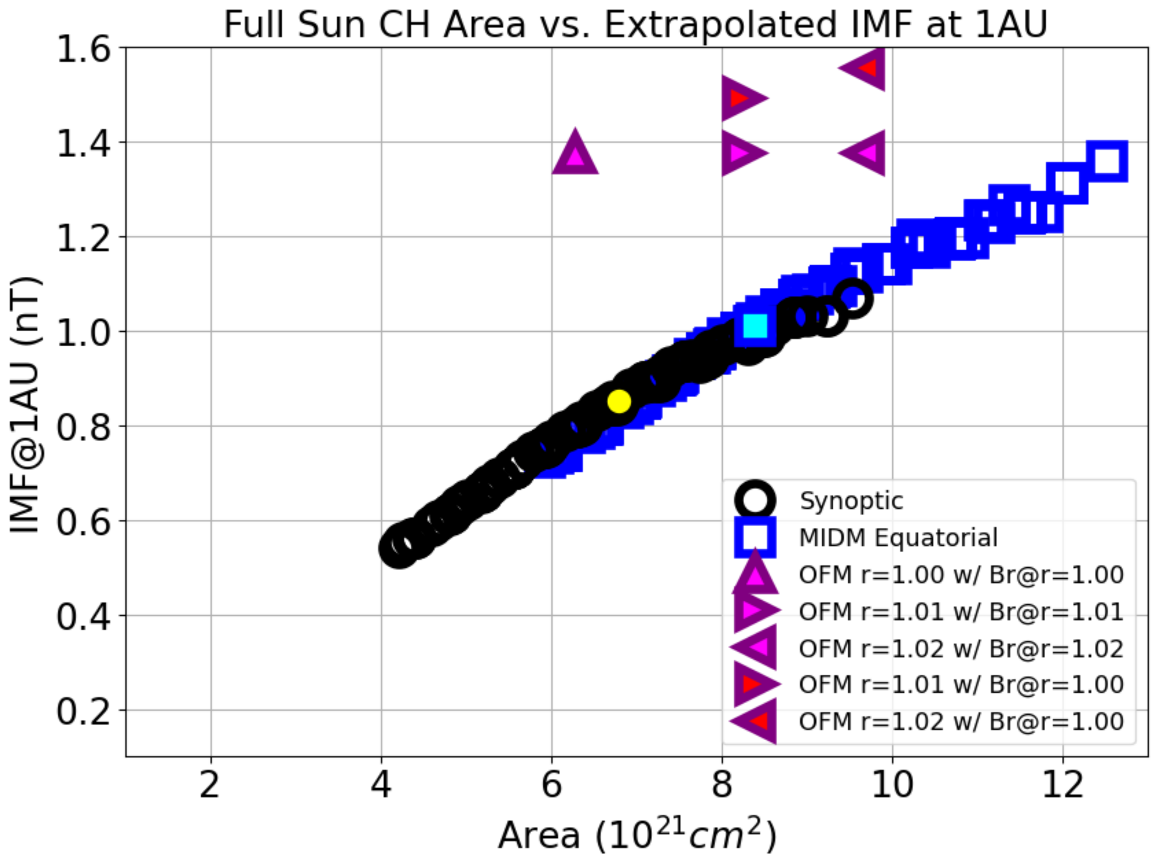

Two key points emerge:

1) The MIDM results are generally both higher area and higher flux than the synoptic results, including the two "best" CH detections. This is due to the greater effect of obscuration near the poles and possibly near bright regions.

2) The true model open flux is higher than most of the reasonable CH detections, even when using MIDM. Looking at the overlaid maps above, one sees that a lot of this flux could be coming from the small open field areas near bright regions that are not dark in the EUV images, or in regions where the open field is near the intensity of the dark quiet Sun, preventing the detection algorithm from capturing them.

OBSERVATIONAL RESULTS

We now apply the MIDM procedure to observations taken during CR 2101.

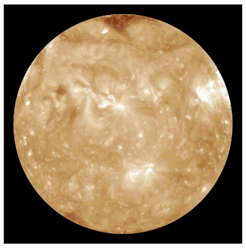

We take 110 disk images from SDO's AIA 193 centered in time within CR 2101. These disk images are then processed with our limb brightening correction method.

The disk images are combined into EUV maps using both the synoptic and MIDM methods. Using the CH detection algorithm EZSEG, we extract an ensemble of CH detections from the EUV maps, and subjectively choose the "best" detection to highlight. This detection for the synoptic EUV map is shown here:

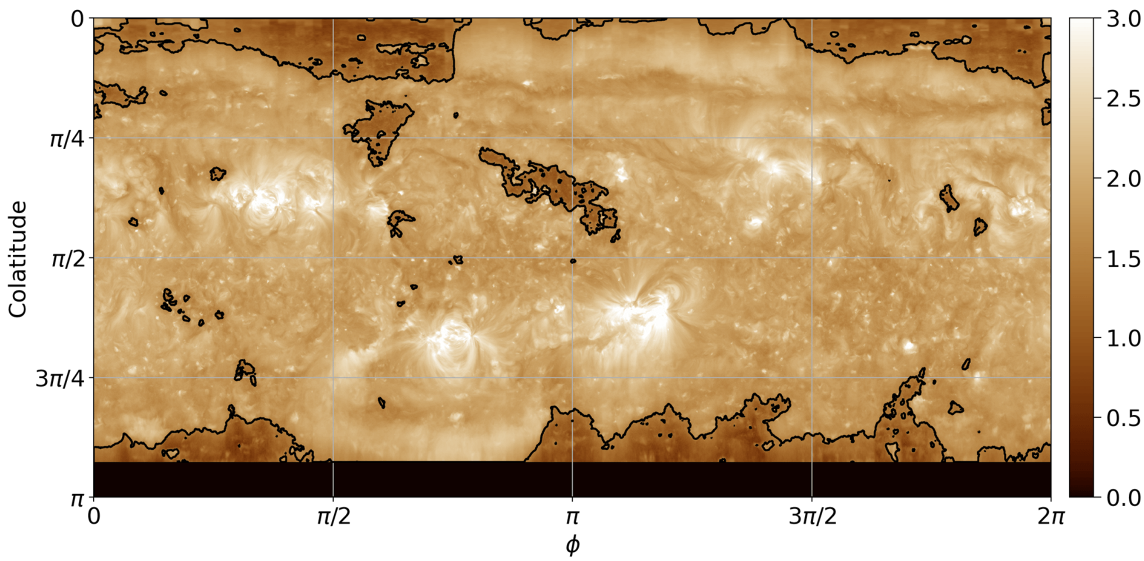

while that for the MIDM EUV map is shown here:

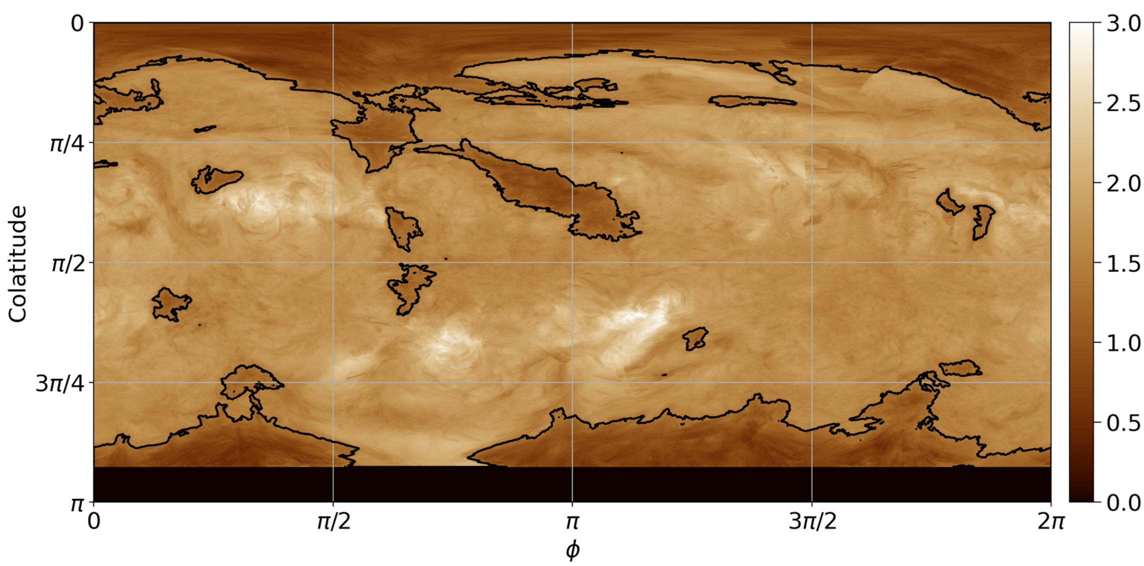

Here, we see more differences between the two methods than in the model case. One reason for this is the fact that the surface structures, including the CHs, are evolving over the CR. The MIDM method thus 'washes out' fine details.

We once again compute flux estimates using the JSOC's pole-filled CR 2101 HMI synoptic map. This time, the map at full resolution with no modifications is used instead of the smoothed map used in the model. This is because, since the CH detections are at high resolution, we want to keep the CH and EUV resolutions similar. The Br map used is shown here:

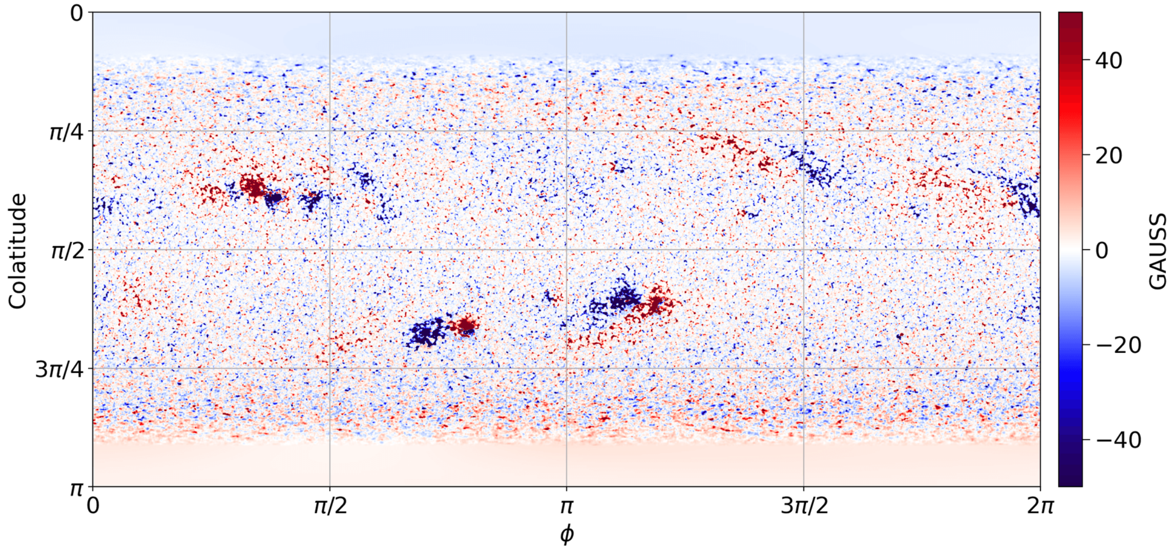

Overlaying the CH from the synoptic EUV map, yields

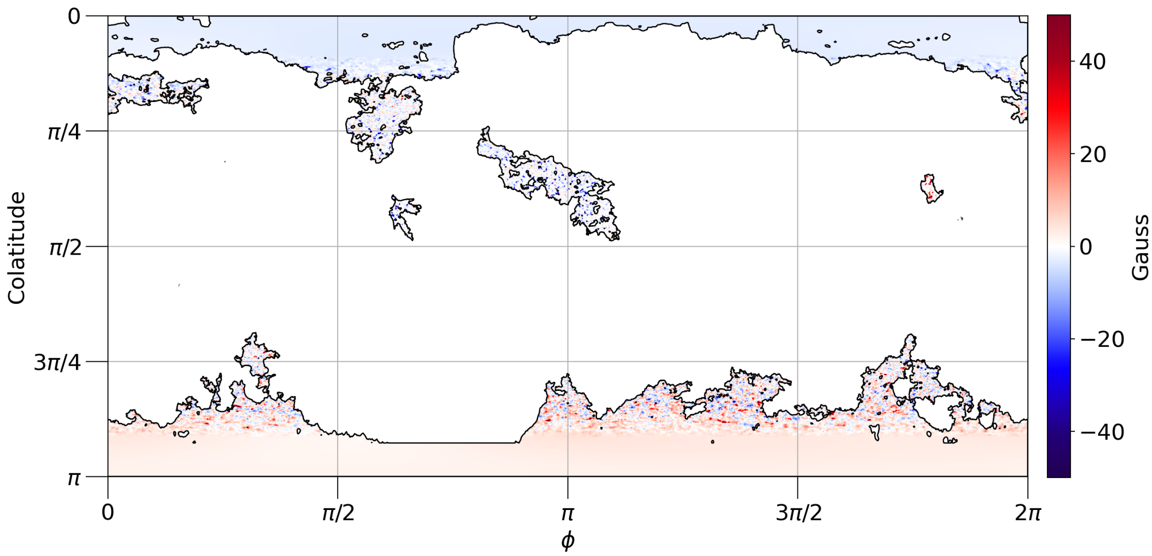

while overlaying the CH from the MIDM EUV map yields

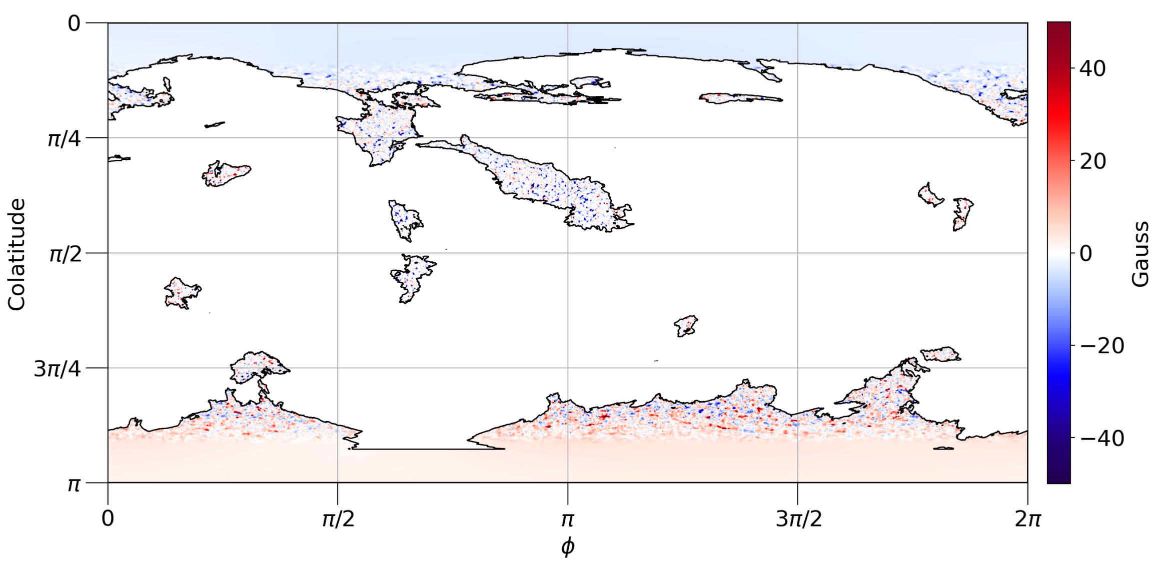

The following two figures show the percentage of open flux within each CH on the map for the synoptic and MIDM EUV maps respectively:

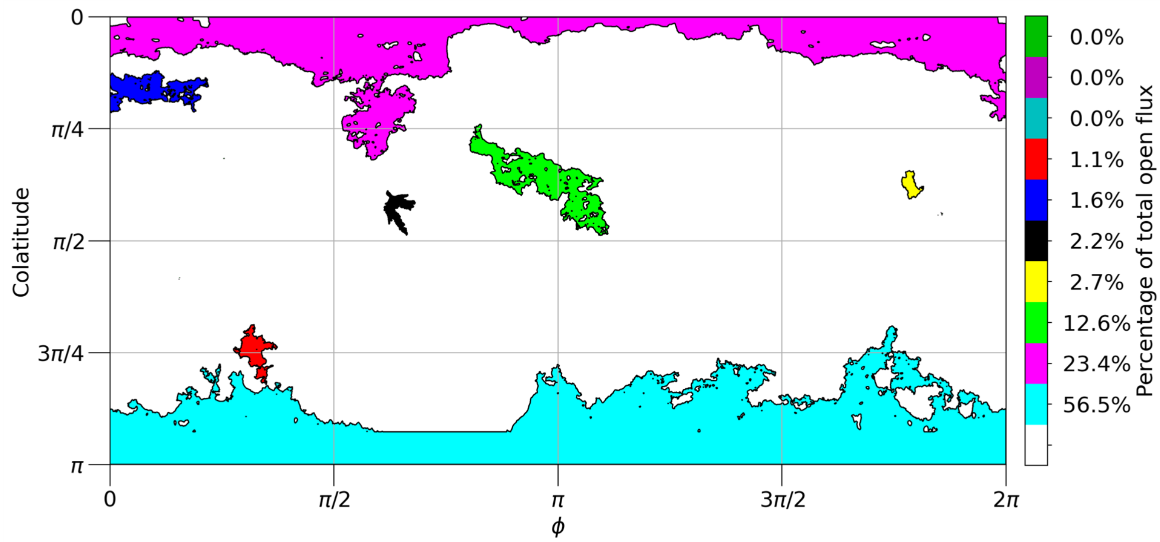

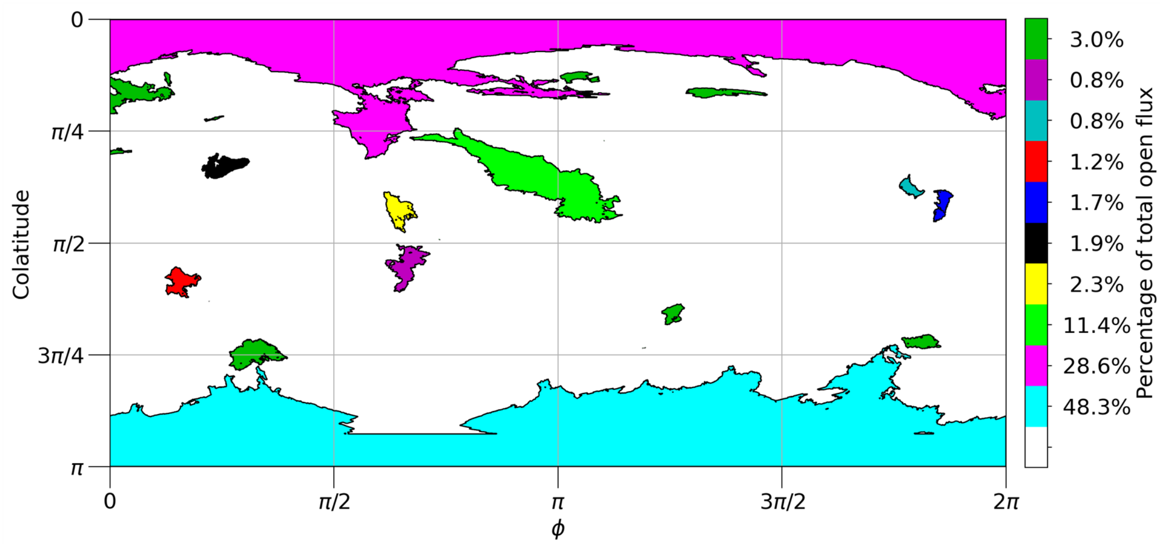

In this case, we have no choice but to use the surface Br data even though the EUV data is at an effective height of ~r=1.01 Rs. Since the effective height is lower than in the model, we expect this miss-match to be less of a problem. We plan to study this in more detail in the future.

The open flux results for only the central equatorial CH are shown here. As in the model case, the yellow-filled circle and the cyan-filled square represent the "best" CH detections.

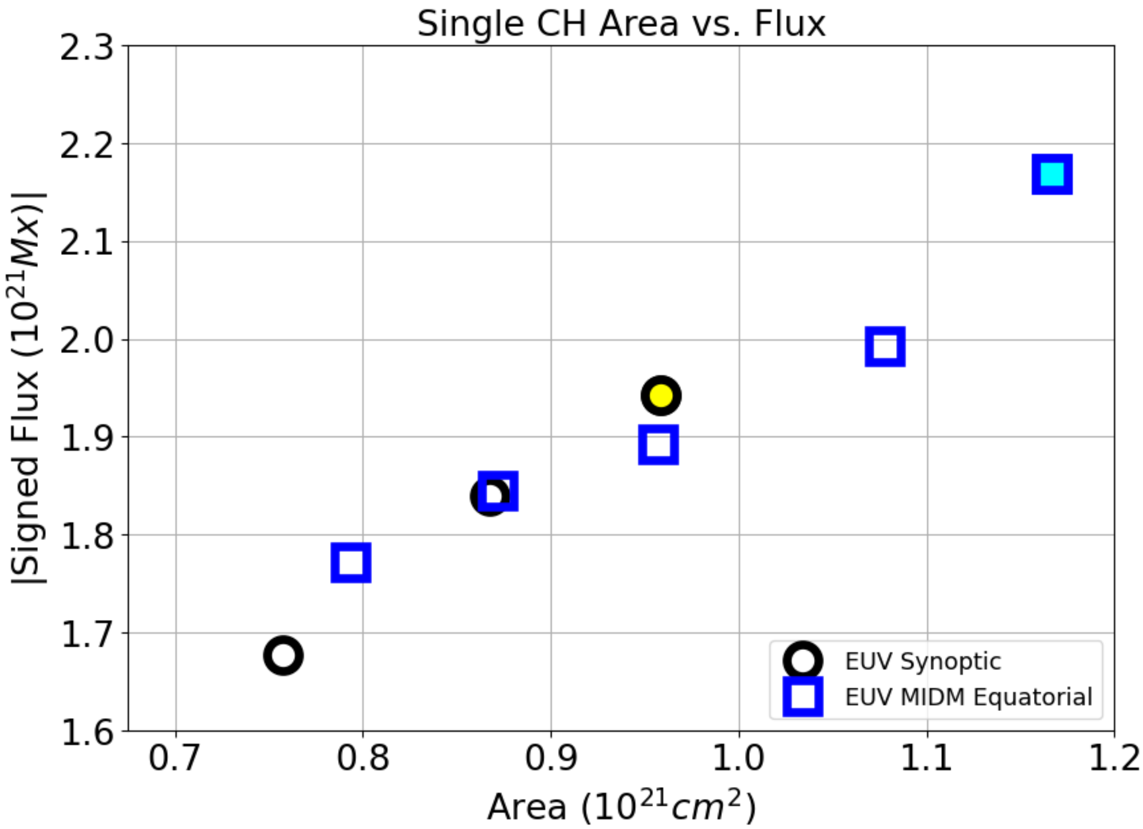

Here we see a much wider spread of areas and fluxes when varying CH detection parameters than we did in the model results. We also see that, unlike in the model case, the MIDM for the central CH generally yields larger areas and fluxes than the synoptic case. This may be due to capturing the evolution of the CH.

For full-Sun results, we set the same southern pole latitude limit as in the model case and get:

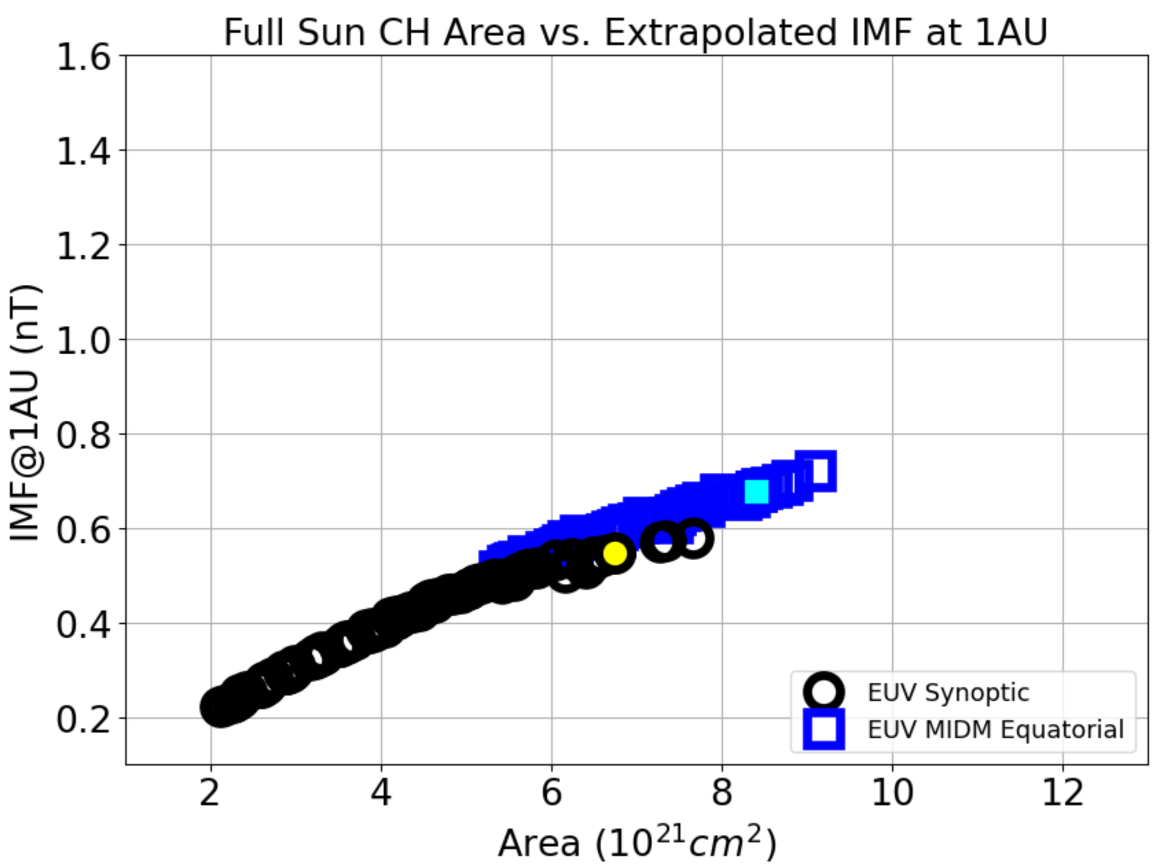

Some key points:

1) The MIDM method consistently produces larger areas and fluxes than the synoptic method. While part of this increase may be due to CH evolution being captured in a "persistence" manner, the model results (where there was no evolution) implies that a significant amount of this increase is due to the MIDM observing CH area that is otherwise obscured.

2) The full Sun CH areas and fluxes are overall lower than those in the model. Interestingly, the "best" detections produce similar areas to the model, but much lower fluxes. This could be due to some CHs or CH extended areas not being visible as dark-enough areas in the EUV maps. Looking at the model results, we saw that the there were many more small equatorial CHs than in the observations. These open field areas (excluding the large central one) accounted for over 40% of the model open flux.

To ensure the difference in open flux is not simply due to the different smoothing/poles of the Br maps, we computed the open flux of the model using the high resolution Br map used here. The resulting IMF differed only 1.5% from the model's open field IMF result with the smoothed/modified Br map.

CONSIDERATIONS

A consideration when using the MIDM method on observational data is coronal hole evolution. Since the MIDM builds up the EUV map from several full disk images, large changes in CH morphology can be combined to make a "persistence map" effect that may result in CH detections being too large. In this case, we used images from a full Carrington rotation. One way to minimize this problem is by using images from other instruments in orbit around the Sun (such as the STEREO spacecraft) so that less time is needed to obtain disk images that cover all longitudinal angles. Also, when studying a specific equatorial CH, less than a full rotation of time can be used.

Independent of the MIDM method, we point out that it may be important to consider the resolutions and/or heights of the EUV and solar surface Br data when using them to estimate open flux. As we saw in the model results, the morphology for the open field is noticeably smoothed out at even low heights above the surface. We also showed that overlaying the detected CHs on the surface magnetogram gave incorrect open field area and open flux results. Although this effect may be less of an issue in observations, it should be considered when combining CH and magnetic data.

SUMMARY

We have introduced the MIDM method for constructing full-Sun EUV maps as an alternative to the classic synoptic method. When using a thermodynamic MHD model, the MIDM method was shown to help mitigate coronal hole obscuration, yielding open flux results that were closer to their true values. It was most helpful near the poles and in areas where coronal holes were adjacent to bright active regions.

Applying the method to observations yielded a coronal hole map that had larger and more numerous detected coronal holes, yielding higher open flux estimates. However, the flux estimates were still quite low overall. We observed that in the MHD model, there were numerous small equatorial open field areas that contributed a large percentage of the total open flux. These areas were difficult to detect in the synthetic EUV images as coronal holes (and in some cases were not detected at all). Such areas (if ubiquitous on the actual Sun) could help explain why the open flux in the observations are low.

We also have shown how the effective height of EUV images can have a non-trivial effect on open flux estimations using solar surface magnetograms.

While the MIDM does not solve all obscuration problems (and can sometimes over-detect CHs due to CH evolution), it shows promise in obtaining more consistent and accurate CH detections from observations. The method may be especially useful during solar maximum where there are many active regions that can obscure equatorial CHs.

ABSTRACT

Coronal holes (CH) are dark areas in EUV images that are generally associated with open magnetic field regions on the Sun. CHs detected over the entire Sun can be used to estimate the open magnetic flux in the heliosphere by overlaying them on magnetic field measurements. Making accurate estimates is difficult due to many factors, including limited instrument coverage, uncertainties in the observations, and challenges in reliable detection of CH boundaries. One such CH detection challenge stems from the fact that EUV line-of-sight observations essentially flatten the three-dimensional structure in the low corona, which can cause nearby bright structures to obstruct CHs.

Here we introduce a mitigation strategy for avoiding the effects of CH obscuration. Using a global thermodynamic MHD model of the corona, we first generate synthetic EUV images for a multitude of observer locations (chosen to mimic the view of SDO over the solar rotation) and combine them into a full-Sun synoptic EUV map. A CH map is then extracted using an established detection algorithm. The resulting open flux estimates are computed and compared to the model's true open flux.

The mitigation strategy (called "minimum intensity disk merge (MIDM)") is applied by changing the way multiple EUV disk images are combined. Instead of using central strips, full disk images are used by taking the minimum intensity in all overlapping regions. This allows any CH area observed at any vantage point to be seen in the final map. We compare the resulting open flux and CH areas to those using the standard synoptic method.

We apply the MIDM method to SDO AIA 193 observational data for the same rotation, and the resulting EUV and CH maps (with corresponding open flux estimates) are compared. Issues such as CH evolution over the rotation, and synchronizing the effective EUV image height to the height of the magnetic field values are discussed.